Proceedings of 10th International Conference on Precision, Meso, Micro and Nano Engineering (COPEN 10)
December 07 – 09, 2017, Indian Institute of Technology Madras, Chennai – 600 036 INDIA

Study of Wire Electro Discharge Machining Accuracy of TiNiCu Shape Memory Alloys through Kerf Analysis

Abhinaba Roy[*1], Narendranath S.[*]

[*]Department of Mechanical Engineering, National Institute of Technology Karnataka, Surathkal, Mangalore - 575025, INDIA

Abstract

Wire electro discharge machining (WEDM) is in use for several decades to process difficult-to-machine materials and are preferred due to its ability to produce micro profiles and reproducible superior machining quality. TiNi based alloys are hard materials and suffer intense surface degradation if machined using conventional machining techniques. These alloys are in widespread use and have great potential for future applications. Alloying of TiNi binary alloy with a ternary element improves its functional quality, which solely depends on the application it is intended for. In this study, TiNiCu inter-metallic alloys ($Ti_{50}Ni_{40}Cu_{10}$ and $Ti_{40}Ni_{50}Cu_{10}$) are chosen due to their ability to retain original shape set at its austenitic phase (shape memory effect) and are currently regarded as potential material for microactuator applications. The primary aim of this study is to quantify the variation in machining accuracy exhibited due to difference in material property under similar machining conditions. Kerf width is considered as the major response to classify the obtained accuracy. It was found that at lower machining rate, kerf width is lower which indicates higher accuracy. But damage to kerf boundary reduces the surface aesthetics and are not only limited to higher machining rate. Percentage accuracy for $Ti_{50}Ni_{40}Cu_{10}$ varies from 60.8% - 81.2% and for $Ti_{40}Ni_{50}Cu_{10}$ it varies from 61.2% - 81.2%. Attempts have been made to find the set of parameters yielding satisfactory accuracy without compromising with volumetric material removal rate. ANOVA helped to determine the most influencing parameters and percentage contribution of each parameters on obtained accuracy.

Keywords: WEDM, Shape memory alloy, Kerf width, Material removal rate

1. INTRODUCTION

Extensive research have been carried out to implement shape memory materials into modern intricate applications. MEMS is one of the fields where TiNi based shape memory alloys are used in thin-film form for micro scale applications which require expensive fabrication costs. However, when macro scale applications are concerned, other suitable manufacturing options can be incorporated. Thin sheet based microgripper, shape and wing morphing, polymer stent using embedded shape memory alloy are some of the applications where components are designed and fabricated using either laser machining or shape memory wire as its elemental structure, as reviewed by Sun et al. [1]. The current study emphasizes on the possibility that there are other numerous applications in macro scale regime which can be manufactured using wire electro discharge machining (WEDM) process. Wire electro discharge machining process has been regarded as the most suitable technique to process difficult-to-machine materials like TiNi based shape memory alloys [2-3]. EDM is limited to profile mirrored by the tool electrode whereas complex two dimensional profiles can be programmed and machined using WEDM. Compared to other machining techniques, WEDM produces components having superior finish and structural integrity. For materials like TiNi based shape memory alloys, accuracy of the part and its metallurgical uniformity has to be maintained after processing. To maintain accuracy in WEDM process, kerf width has to be minimum. Researchers have been working on parametric optimization of kerf width to enhance the accuracy of WEDMed part [5-7]. On the other hand, formation of recast layer is associated with formation of micro-cracks on the machined surface which may lead to failure of the machined component in the long run [8]. Therefore, it is required to reduce the recast layer thickness to avoid complications.

Due to narrow hysteresis compared to binary TiNi alloy, TiNiCu alloy can be used for actuation purpose for longer cycles. TiNiCu shape memory alloy has been studied extensively due to special "two-way shape memory effect" [4], in which a spring can contract while being heated and expand while cooled. MEMS industry depends on various types of microactuators and sensors to perform operations like microassembly and micromanipulation. Microgrippers are widely used to hold miniature parts and shape memory alloys qualify as ideal material where it can be energized to generate heat and perform suitable movement by displacing its jaws. In this study, TiNiCu shape memory alloy $Ti_{50}Ni_{40}Cu_{10}$ and $Ti_{40}Ni_{50}Cu_{10}$ were selected based on favorable characteristics like lower critical stress for slip, low thermal hysteresis, two-stage transformation [9-11] and machined using WEDM. It is widely known that WEDM is associated with numbers of issues regarding the quality of the machined surface and some of them are already addressed in our previous work [3, 12, 13]. Surface and subsurface quality also gets affected which are also equally responsible for the functional integrity of the WEDM processed material. Although extensive research work is carried out in kerf analysis of silicon wafers [15], very few of them discussed about kerf width variation due to the difference in physical properties of the alloys selected in current investigation. The current study aims at quantifying the variation in response and underlying basis for such behavior.

2. MATERIALS AND METHODS

Two separate TiNiCu alloys ($Ti_{50}Ni_{40}Cu_{10}$ - TNC1 and $Ti_{40}Ni_{50}Cu_{10}$ - TNC2) were prepared using vacuum arc melting. The obtained ingot bars were melted and re-melted six times each to maintain homogeneity and further homogenized at 500°C for 1 hour. Thereafter, the bars were prepared for kerf width study by profiling out a rectangular block. Surface roughness samples were prepared separately by slicing another set of ingot bars (Ref Fig. 1).

[1]Corresponding author, er.abhi.roy@gmail.com, +91-7022384560

ISBN: 978-93-80689-28-9

Fig. 1. (a) Rectangular profile for kerf study (b) TiNiCu ingot bar (c) Surface roughness sample

Taguchi's L16 orthogonal array was implemented in this investigation to study the effect of machining process parameters on variation of kerf width. At four levels of varying process parameters, L16 was the only available experimental design as per Taguchi's design of experiment. Parameters were selected based on machine capability which was a Electronica India Ltd. manufactured ELPULS15 wire electro discharge machine. Selected parameters were pulse on duration (T_{on}), pulse off duration (T_{off}), servo voltage (SV) and wire feed rate (WF), which were varied at four levels and their consequent effect was observed on variation of kerf width. For kerf width study, slits of 2 mm were cut for each of L16 experiments. Schematic of kerf width profile is shown in Fig. 2 and volumetric material removal rate (VMRR) is calculated based on depicted profile and Equation 1.

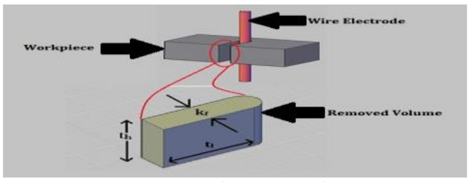

Fig. 2. Kerf width profile

$$VMRR=\frac{[(t_l \times t_h \times k_f)+\frac{\pi}{2}\times\left(\frac{k_f}{2}\right)^2\times t_h]}{T} \quad (mm^3/min)$$
(1)

Where, $\mathbf{t_l}$ = travel length (mm), $\mathbf{t_h}$ = workpiece thickness (mm)
$\mathbf{k_f}$ = kerf width (mm), **T** = time taken (minutes)

Surface roughness of the L16 experiments were obtained from the slices obtained from the samples as shown in Figure 1c. The surface roughness of the machined surfaces are noted using Mitutoyo SJ-301 surface roughness tester. For better accuracy, the surface roughness denoted, is the arithmetic mean of each sample measured at six different locations. 0.25mm/s was considered as the stylus speed and an evaluation length of 4.0 mm was kept constant for each sample.

3. RESULTS AND DISCUSSIONS

3.1 Effect of process parameters on Kerf Width

Accuracy of a component machined using WEDM can be quantified in terms of kerf width which is the gap created by the wire electrode after it has traversed a certain position. Collectively, wire diameter and spark gap on the both sides of the wire contribute to the kerf width. Spark gap is determined by the input process parameters of the WEDM process which varies depending on the parameter values. In this study, pulse on time (T_{on}), pulse off time (T_{off}), servo voltage (SV) and wire feed (WF) were varied to study their influence on kerf width. It can be observed from Fig. 3a that kerf width increases as pulse on duration (T_{on}) extends for the selected alloys and can be explained by the fact that a rise in discharge duration melts more material resulting to a wider kerf hence lower accuracy. Fig. 4 clearly establishes the effect of increasing pulse on duration on kerf width as more re-solidified molten debris are present along the kerf boundary due to increasing explosive nature of the molten material. Tosun et al. [5] also investigated variation in kerf based on Taguchi method and reported similar characteristics.

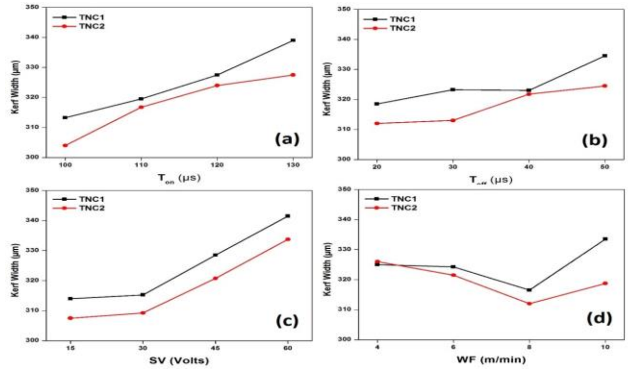

Fig. 3. Kerf width vs. (a) Ton (b) Toff (c) SV (d) WF

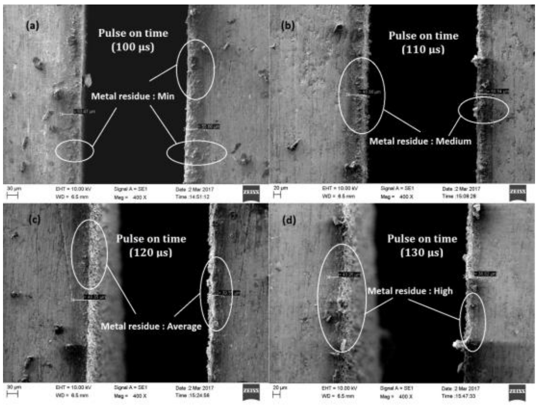

Fig. 4. Kerf width at T_{on} (a) 100µs (b) 110µs (c) 120µs (d) 130µs

Kerf width increases with the extension of pulse off duration (as noted in Fig. 3b) which signifies that due to extended duration of discharge-less period, more molten metal was flushed out. However, it can be observed that at 40µs kerf width value converges for all the selected alloys which indicates that over a certain duration of pulse off time, kerf width can be controlled. Overall effect of pulse off time on kerf width is insignificant compared to other parameters as the net change for initial to final value of pulse off time is not much and is also established by Ikram et al. [7]. Effect of servo voltage in Fig 3c clearly indicates that lower value of servo voltage yields minimum kerf width. Beyond 30 V, kerf width widens abruptly which is due to large ionization of dielectric fluid present between the working gap which is in accordance with the findings of Shichun et al. [6]. Collectively it is evident that effect of servo voltage is influential like it was in case of pulse on duration and can be observed in Fig. 5. Also, larger amount of re-solidified molten debris at kerf boundary can be observed at higher value of servo voltage which establish the effect of larger ionization of dielectric fluid resulting in more molten material. Furthermore, it is evident from Fig. 3d that wire feed rate of 8 m/min surprisingly lowers kerf width and beyond that it widens (at 10 m/min). This behavior is similar for all the selected alloys. It can be observed that variation of kerf width at both 4 m/min and 6 m/min are negligible and it narrows down at 8 m/min. The reason behind such sudden reduction in kerf width at 8 m/min is due to increased wire tension at higher wire feed rate. However, at higher wire feed rate (10 m/min), abrupt wire vibration came into play and widened the kerf. Tosun et al. [5]

also observed similar behavior. This emphasizes the need for proper wire feed selection in maintaining narrow kerf width. The behavior of TNC11 and TNC12 varies under similar machining conditions. This is due to lower thermal conductivity of TNC1 compared to TNC2. Due to lower thermal conductivity of TNC11, it was difficult for this alloy to distribute the local thermal heating by electrical discharge to the nearby TiNiCu matrix and resulted in fast melting of material where discharge sparks localizes hence wider kerf formation. Similar results were observed by Hsieh et al. [14].

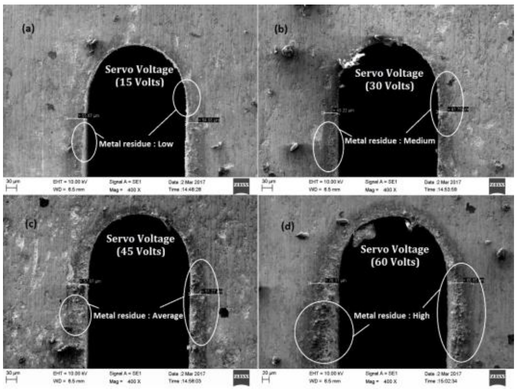

Fig. 5. Kerf width at SV (a) 15 V (b) 30 V (c) 45 V (d) 60 V

3.2 Comparison of machining accuracy based on process parameters

A compact assimilation of kerf width and volumetric material removal rate of the selected alloys for Taguchi's L16 orthogonal experiments have been represented in Fig. 6. From these histograms, it would be easier to apprehend the variation in kerf width under similar machining parameters for the selected alloys and to determine the set of parameters for individual alloy to minimize the kerf width which in turn stands for higher machining accuracy. Diameter of the wire electrode used during machining was 250 µm zinc coated brass wire, therefore kerf width value of a particular experimental run bearing value closer to 250 µm resembles higher machining accuracy. Alongside kerf, the operator should also pay heed to the productivity of the machining process. Therefore, if VMRR is too low but kerf is minimum, that should be reserved for micromachining whereas a little compromise on kerf associated with better material removal rate can be used for producing parts that don't require ultra precision and not bound by tight tolerance limits. For the ease of understanding, these two histograms are divided into four categories depending on the VMRR value which are category 1, 2, 3 and 4. The details are given in Table 1.

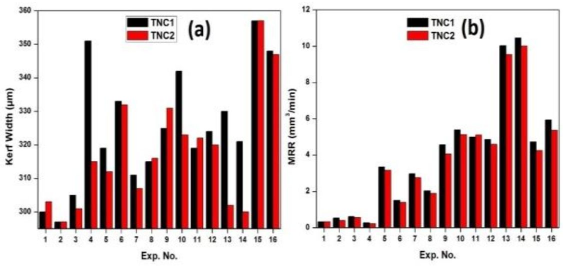

Fig. 6. (a) Kerf width (b) VMRR

Table 1: Categorical classification of obtained kerf width

Category	Experimental Run				Range of VMRR(mm^3/min)
1	1	2	3	4	0-1
2	5	6	7	8	1-4
3	9	10	11	12	4-6
4	13	14	15	16	6-12

For alloy TNC1 and TNC2, least recorded kerf width is 297 µm which was noted at second experimental run of category 1. But the material removal rate for second experimental run is much lower compared to the entire L16 experiments. However, if fifth and seventh experimental runs of category 2 are compared, it can be seen that seventh experimental run is more suitable for smaller kerf width even though VMRR will be compromised in this particular case and is applicable for the chosen alloys. From the micrograph it can be observed that in category 3, eleventh experimental run scores high for machining accuracy whereas it ranks second for VMRR which is considerable compared to other three experimental runs. Even though experimental run thirteen and fourteen exhibit quite smaller kerf and high VMRR, due to extreme damage to the material surface these are not practical options and hence qualify sixteenth experimental run as a more useful option under category 4. For confirmation of the above claims, SEM micrograph of kerf width for second, seventh, eleventh and sixteenth experimental run is shown in Fig. 7.

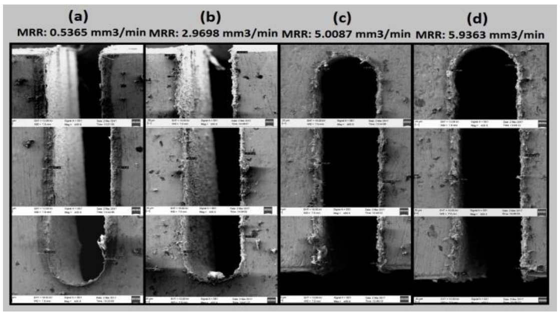

Fig. 7. Kerf width profile of (a) 2nd (b) 7th (c) 11th (d) 16th experimental run

These qualifying set of parameters that succeed to provide a fair machining accuracy, their categories, input process parameters and percentage accuracy are depicted in Table 2.

Table 2: Qualifying kerf width and percentage accuracy

Sl. No.	Experimental Run	Category	Percentage Accuracy
1	2	1	TNC1-81.2% TNC2-81.2%
2	7	2	TNC1-72.4% TNC2-75.2%
3	11	3	TNC1-72.4% TNC2-71.2%
4	16	4	TNC1-60.8% TNC2-61.2%

3.3 ANOVA of Kerf Width

In this section analysis of variance of the obtained results for TNC1 and TNC2 are performed based on kerf width. F-test and P-test values are included in the tables below to find out the influential parameters and their percentage contribution on the selected responses. 95% confidence level is considered while performing ANOVA analysis of the machining responses. Table 3 and Table 4 represents the ANOVA results for TNC1 and TNC2 respectively. In both cases, servo voltage (SV) was found to be the most influential parameter to control kerf width followed by pulse on time (T_{on}). In case of TNC1, servo voltage had 43.32% contribution in influencing kerf width and 43.52%

in case of TNC2. Pulse on time regulates the duration for which the electrical spark discharge is allowed and servo voltage helps in maintaining a constant spark gap. Higher value of servo voltage represents a wider spark gap and therefore lower value of servo voltage yields higher chances of wider kerf formation. It is interesting to note that servo voltage is more dominant in case of kerf width where its percentage contribution is more than pulse on time in the case of all the two alloys selected. Therefore, proper usage of servo voltage is important to maintain a narrow kerf during machining and is especially more important to take control of during corner cutting.

Table 3: ANOVA results for TNC1

Source	DF	Alloy TNC1				
		SS	MS	F	p	P(%)
Ton	3	1481.7	493.90	8.25	0.058	32.07
Toff	3	557.7	185.90	3.10	0.189	12.07
SV	3	2001.7	667.23	11.14	0.039	43.32
WF	3	579.7	193.23	3.23	0.181	12.55

Table 4: ANOVA results for TNC2

Source	DF	Alloy TNC2				
		SS	MS	F	p	P(%)
Ton	3	1222.7	407.6	2.97	0.197	30.08
Toff	3	468.7	156.2	1.14	0.458	3.84
SV	3	1769.2	589.7	4.30	0.131	43.52
WF	3	604.7	201.6	1.47	0.379	14.87

4. CONCLUSIONS

Experimental investigation on wire electro discharge machining of $Ti_{50}Ni_{40}Cu_{10}$ and $Ti_{40}Ni_{50}Cu_{10}$ as cast shape memory alloys has been carried out and following conclusions have been drawn:

- $Ti_{50}Ni_{40}Cu_{10}$ exhibited superior affinity for wider kerf formation and higher material removal rate under similar machining conditions compared to $Ti_{40}Ni_{50}Cu_{10}$ which can be attributed to lower thermal conductivity value of $Ti_{50}Ni_{40}Cu_{10}$.
- For a medium to average VMRR, experimental run 7 and 11 are found to be yielding satisfactory accuracy for kerf width and suitable for machining with average accuracy applicable for the chosen alloys.
- As per ANOVA results, servo voltage (SV) followed by pulse on time (T_{on}) are proved to be most influential parameters when kerf width is concerned.

ACKNOWLEDGEMENT

This experimental research study is funded by Department of Science & Technology, Government of India under the project bearing sanction number SB/S3/MMER/0067/2013. The authors would like to express their gratitude to DST-SERB for its funding support.

References

[1] L. Sun, W.M. Huang, Z. Ding, Y. Zhao, C.C. Wang, H. Purnawali, C. Tang. Stimulus-responsive shape memory materials: A review. Materials and Design; 33:577-640. 2012

[2] M. Manjaiah, S. Narendranath, S. Basavarajappa. Review on non-conventional machining of shape memory alloys. Transaction of Nonferrous Metals Society of China; 24:12-21. 2014

[3] Manjaiah, M., Narendranath, S., & Basavarajappa, S. A Review on Machining of Titanium based alloys using EDM and WEDM. Rev. Adv. Mater. Sci, 36(2), 89-111. 2014

[4] Z.G. Wang, X.T. Zu, X.D. Feng, S. Zhu, J.Y. Dai, L.B. Lin, L.M. Wang. Study of two-way shape memory extension spring of narrow hysteresis TiNiCu shape memory alloys. Materials Letters; 56:284-288. 2002

[5] N. Tosun, C. Cogun, G. Tosun. A study on kerf and material removal rate in wire electrical discharge machining based on Taguchi method. Journal of Materials Processing Technology; 152:316-322. 2004

[6] D. Shichun, C. Xuyang, W. Dongbo, W. Zhenlong, C. Guanxin, Liu Yuan. Analysis of kerf width in micro-WEDM. International Journal of Machine Tools & Manufacture; 19:788-792. 2009

[7] A. Ikram, N.A. Mufti, M.Q. Saleem, A.R. Khan. Parametric optimization for surface roughness. kerf and MRR in wire electrical discharge machining (WEDM) using Taguchi design of experiment. Journal of Mechanical Science and Technology; 27(7):2133-2141. 2013

[8] Aspinwall, D.K., Dewes, R.C., Lee, H.G., Simao, J., McKeown, P.A. Electrical Discharge Surface Alloying of Ti and Fe Workpiece Materials Using Refractory Powder Compact Electrodes and Cu Wire. CIRP Annals-Manufacturing Technology; 52(1): 151-156. 2003

[9] W.J. Moberly, J.L. Proft, T.W. Duerig, R. Sinclair. Materials Science Forum; 56-58:605-610. 1990

[10] H.J. Yu, Z.G. Wang, X.T. Zu. Temperature memory effect in two-way shape memory TiNi and TiNiCu springs. Journal of Materials Science; 41:3435-3439. 2006

[11] A. Ishida, M. Sato, Z.Y. Gao. Properties and applications of TiNiCu shape memory alloy thin films. Journal of Alloys and Compounds; 577S: S184-S189. 2013

[12] Manjaiah, M., Narendranath, S., Basavarajappa, S., & Gaitonde, V. N. Wire electric discharge machining characteristics of titanium nickel shape memory alloy. Transactions of Nonferrous Metals Society of China, 24(10), 3201-3209. 2014

[13] Manjaiah, M., Narendranath, S., Basavarajappa, S., & Gaitonde, V. N. Effect of electrode material in wire electro discharge machining characteristics of Ti50Ni 50−xCux shape memory alloy. Precision Engineering, 41, 68-77. 2015

[14] S.F. Hsieh, S.L. Chen, H.C. Lin, M.H. Lin, S.Y. Chou. The machining characteristics and shape recovery ability of Ti-Ni-X (X = Zr, Cr) ternary shape memory alloys using the wire electro-discharge machining. International Journal of Machine Tools and Manufacture; 49:509-514. 2009

[15] Kamlesh Joshi, A. Ananya, Upendra Bhandarkar, Suhas S. Joshi, Ultra thin silicon wafer slicing using wire-EDM for solar cell application. Materials & Design; 124:158-170, 2017